ACS APPLIED MATERIALS & INTERFACES

Research Article

www.acsami.org

Patterning of Two-Level Topographic Cues for Observation of Competitive Guidance of Cell Alignment

Xiongtu Zhou,[†,‡] Jie Hu,[†] Junjun Li,[†] Jian Shi,[†,*] and Yong Chen[†,§,*]

[†]Ecole Normale Supérieure, CNRS-ENS-UPMC UMR 8640, 24 rue Lhomond, 75231 Paris, France

[‡]College of Physics and Information Engineering, Fuzhou University, 350002 Fuzhou, China

[§]Institute for Integrated Cell-Material Science, Kyoto University, Kyoto 606-8507, Japan

Supporting Information

ABSTRACT: Cells display contact guidance when cultured on topographical cues. By combining standard photolithography, nanoimprint lithography, and soft lithography, we produced sophisticated patterns on two levels, including crossing microgrooves with different depth/spacing and microgrooves with superimposed submicrometer features. The results show that for narrowly spaced microgrooves, the contact guidance is more significant to the change of groove depth than to other geometry parameters. For crossing microgrooves, the shallow grooves take over the influence on cell alignment when the deeper grooves are well separated. Finally, the superimposed submicrometer features on the groove ridges decrease the efficiency of the contact guidance of microgrooves, due to increased adhesion of cells on patterned surfaces.

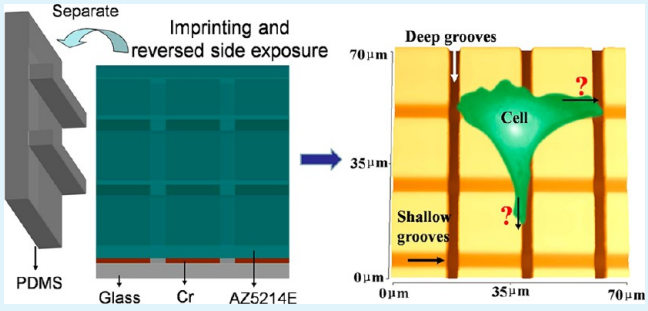

KEYWORDS: *cell alignment, cell−substrate interaction, two-level topographic cues, microgroove*

INTRODUCTION

The control of cell-material interaction is of great importance in tissue engineering.[1−3] Micro- and nanotopographic patterns are now widely used to mimic the structural and mechanical properties of in vivo extracellular matrix (ECM).[4−8] Among many others, patterned microgrooves are typical examples of topographic features showing strong effect of cellular contact guidance.[3,9−12] However, previous studies were mainly based on one-level patterns which could be easily produced by standard lithography methods but may not fully take into account the morphological complexity of the extracellular matrix. Indeed, cells in a real tissue are subject to an environment of three-dimensional space, multiple soluble factors, and cell−cell interactions. In response to stimuli in a dynamic and complicated manner, cytoskeleton can be remodeled, and cells can migrate toward the more favorable sites.[13−16] This requires more detailed investigations by considering, for example, topographic patterns of more complex layout and eventually three-dimensional design of biomimic architectures.

Mai et al. recently studied cytoskeleton dynamics using multidirectional topographical cues.[17] The grid-patterned substrates were also used to control directional migration of cells, showing that both cell shape and displacement are exquisitely sensitive to local anisotropy and that cells could integrate orthogonal spatial cues when determining the direction of cell orientation and movement.[18,19] These findings have provided valuable insight into cellular responses to multidirectional stimuli. However, these stimuli were still limited in two dimensions. Recently, there are more and more reports on the cell contact guidance on scaffolds in three dimensions as described in a review article by Nikkhah et al.;[20] however, those fabrication methods of 3D scaffolds were mostly based on stereolithography and two-photon absorption lithography, which are still cost-ineffective and time-consuming, and have not been extensively used to generate topographies for biological studies. Furthermore, a preferred fabrication technique should be capable of producing both large and small features in various combinations and distributions, providing higher degree of biomimetic relevance, which is also a typical requirement in biological applications. Thus, it is still challenging to fabricate high resolution and three-dimensional cues on demand by using current technologies.[3,12,21,22]

In this work, we introduce a simple but yet robust and versatile combination of lithographic methods to produce multilevel topographic patterns for cell culture studies. Conventional photolithography, nanoimprint lithography, and soft lithography were combined to fabricate two-level crossing grooves and other types of patterns with different feature sizes, spacing, and depths. The fabricated samples were then used to study cellular responses to these multilevel cues.

Received: April 12, 2012
Accepted: July 27, 2012
Published: July 27, 2012

 © 2012 American Chemical Society

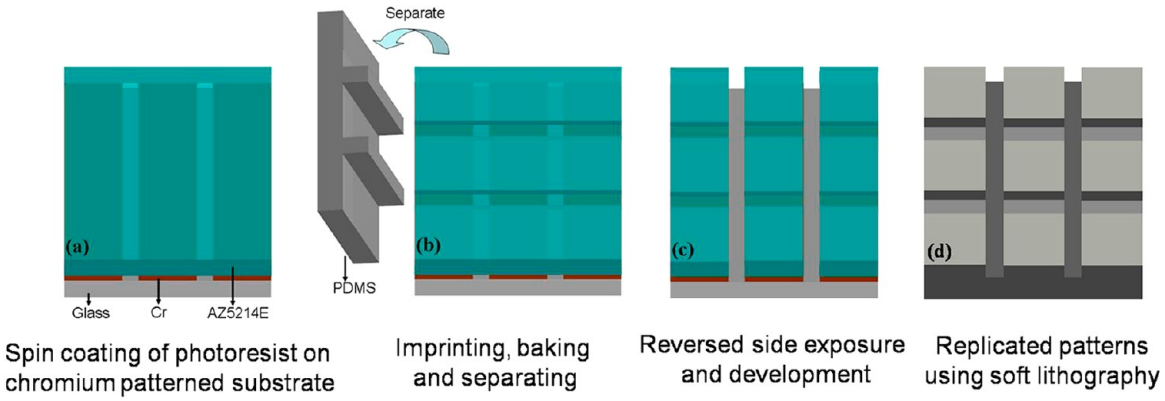

Figure 1. Schematic illustration of the fabrication process by combining nanoimprint and photolithography to define two-level topographic patterns (a–c). The resulted patterns can then be replicated twice by soft lithography with a biocompatible material such as polymethylsiloxane (d).

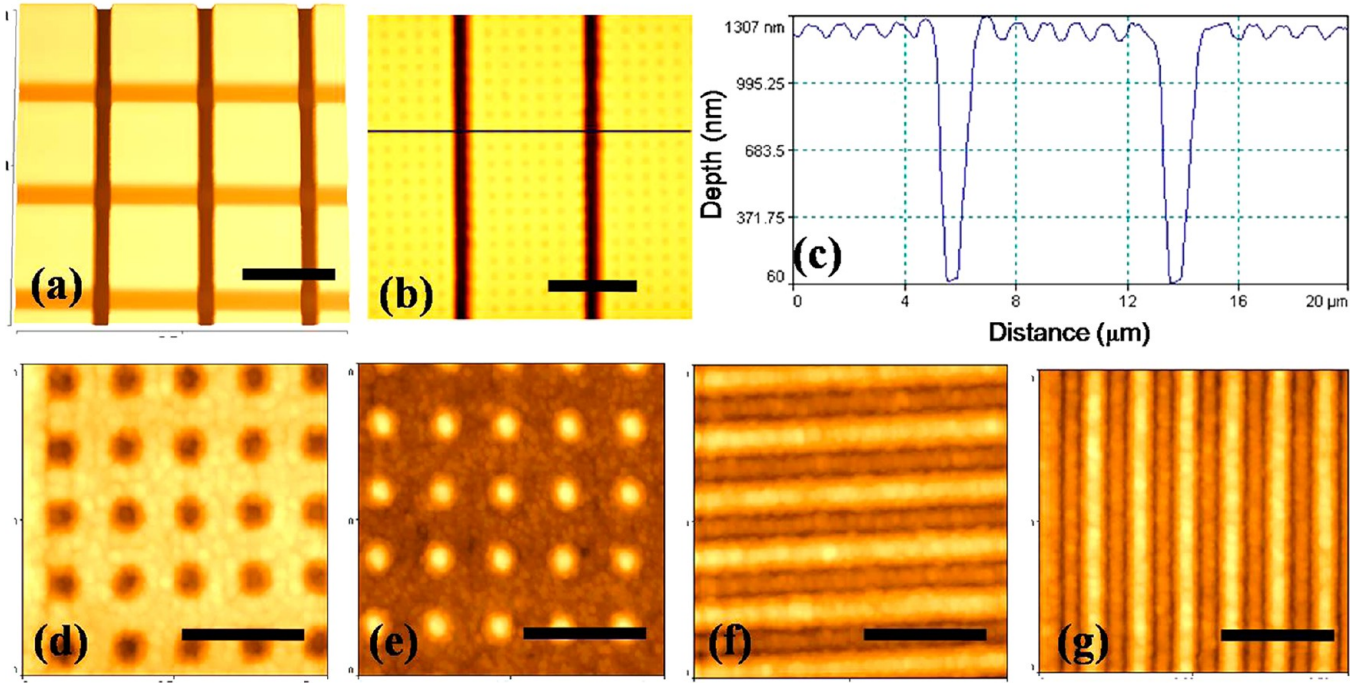

Figure 2. Two-level topographic cues for cell culture studies. (a) AFM image of crossing grooves with depths of 0.7 μm (light) and 1.4 μm (dark) in two different directions. (b–c) AFM image and line profile of microgrooves superimposed with nanopits on the ridges. (d) Zoomed view of (b). Other features such as nanopillars (e) and nanogratings perpendicular (f) or parallel (g) to the microgrooves. Scale bar: (a) 20 μm, (b) 5 μm, (d–g) 2 μm.

MATERIALS AND METHODS

Fabrication of Multilevel Patterns. The fabrication process of the multilevel patterns used in this work is schematically shown in Figure 1. First, the designed bottom level pattern was defined by direct laser writing (DLW) using a micropattern generator (μPG 101, Heidelberg Instruments) on a chromium plated soda lime glass plate of 3 mm thickness precoated with AZ1518 photoresist (Nanofilm, Wetlake Village, California). After exposure and development, the pattern was transferred into the Cr layer by wet etch in a chrome etchant solution (chrome-etch 3144, Honeywell), leaving a clear path to light. The residual photoresist was then removed by acetone. Afterward, AZ5214E photoresist (Cipec, France) was spin coated at a speed of 4000 rpm on the Cr pattern (Figure 1a), immediately followed by nanoimprint lithography with a mold made of polydimethysilaxane (PDMS). Here, the PDMS mold was obtained by casting with a master mold fabricated by other lithography techniques such as photolithography, electron beam lithography, and so forth, depending on the resolution requested.[23,24] The substrate, together with the mold, was baked on a 125 °C hot plate for 80 s. After cooling down, the PDMS mold was peeled off from the substrate, resulting in the top-level pattern on the surface of the resist layer, as seen in Figure 1b. By controlling the feature height of the PDMS mold as well as the pressure of the nanoimprint, the residual thickness of the resist or the depth of imprinted top-level feature could be changed, but it is less than the total thickness of the resist. Finally, the imprinted resist layer was exposed by UV light from the reversed side of the substrate. After development, the regions exposed to UV light were removed, resulting in another pattern superimposed to the imprinted one with different thickness (Figure 1c). In order to study cell responses to two-level cues, different types of patterns were produced and then replicated by using soft lithography (Figure 1d).

Cell Culture and Seeding. The molded PDMS layers were washed in pure ethanol and DI water, dried with nitrogen, and sterilized in an autoclave (Subtil Crepieux, France). Afterward, the samples were baked in an oven at 80 °C overnight for next step use. Since the effect of increasing the hydrophilicity using O_2 plasma can only stand for 5–10 min, the substrates should be passed for O_2

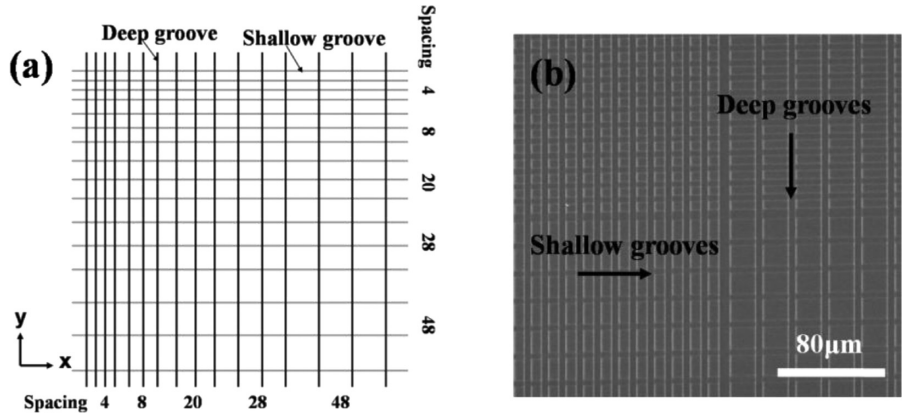

Figure 3. Schematic (a) and SEM image (b) of a fabricated crossing-groove pattern with different groove depths and spacings.

plasma treatment after sterilization, and then passed immediately for protein coating and cell culture before cell seeding. Concretely, the samples were treated with O_2 plasma for 3 min to increase the hydrophilicity immediately followed by dipping them in fibronectin (FN, Sigma) solution with bulk concentrations of 25 μg/mL for 40 min under room temperature and then washed in PBS for three times to remove unbound proteins.

NIH 3T3 cells were cultured in DMEM (Gibco) supplemented with 10% fetal bovine serum, 1% penicillin/streptomycin, 1% L-glutamine, and 0.01% fungizone (Sigma-Aldrich, France). Cells were dissociated with 0.05% Trypsin EDTA solution at 37 °C for 3 min. The fabricated PDMS substrates were put into six-well plate (Fisher Scientific, France) seeded with a final concentration of about 10 000 cells/cm^2.

Cell Imaging and Statistic Analysis. Cells were cultured for about 20 h prior to performing measurements. After rinsing in PBS for the removal of unattached and dead cells, the cells were fixed with 4% formaldehyde in PBS solution for 30 min. After that, cells were permeabilized in 0.5% Triton-X-100 PBS solution for 10 min, blocked in a PBS solution with 3% BSA and 0.1% Triton-X-100 for 30 min, incubated with Phalloidin-FITC (1 μg/mL) and DAPI (100 ng/mL) for 20 min, and finally washed three times with PBS.

The specimens were examined using a fluorescent microscope (20x, ZEISS Axiovert 200) equipped with a B&W CCD camera (Evolution QEi, Canada). We were particularly interested in cellular contact guidance on patterned two-level grooves. Three to five images (850 μm × 650 μm) were taken from different parts of each pattern, and the cell orientation on each kind of microgroove was determined from at least 300 cells to get the mean values. Microscope images were processed using ImageJ (version 1.41, NIH). The cell nucleus was fitted with an ellipse and the angle (θ) of the major axis with respect to the shallower microgroove direction was taken. Three sets of experiments were conducted; the final data were calculated from the mean value of three sets (each set has a mean value to represent the value of this set), and all data are presented as mean ± standard deviation.

RESULTS AND DISCUSSION

Our two-level patterning method is efficient and cost-effective, since different micro- and submicrometer patterns could be generated by using a limited set of chrome masks and a PDMS mold. Although the minimum pattern size that this technique could manage in this work is about 400 nm, this method is robust compared to more conventional fabrication of quartz or silicon multilevel patterns, which generally require metal deposition and dry etching,[25] and we believe that the size limit of this technique might be explored smaller by adjusting the parameters such as the printing pressure and the viscosity of the photoresist. In addition, it is more flexible to design different types of hybrid patterns with various structural compositions, sizes, and geometries. Figure 2 shows AFM images of a few of fabricated patterns, proving that not only microstructures but also submicrometer structures could be produced in AZ5214E photoresist with a high resolution. In vivo, ECM often forms interlinked structures of variable densities at multi levels. To investigate how cells respond to such meshworks, we designed several types of cell culture substrates. Figure 3 shows a test pattern of two-level grooves with the same width (4 μm) but variable spacing in the range between 4 and 48 μm. From the AFM measurement, the groove depths of about 1.4 μm in the y direction and 0.7 μm in the x direction were determined. This type of pattern can exert contact guidance in three dimensions with different efficiencies in the x, y, and z (depth) directions, depending on the grid aspect ratio and the groove depth. For the range of our investigation, the size of a unit grid was smaller than that of a single cell so that each cell experiences simultaneous contact guidance leading to different directions.

NIH 3T3 fibroblasts were cultured on fibronectin-coated topographic substrates for 20 h. The morphology of the cells on different aspect ratio and grid patterns with respect to their orientation was characterized based on fluorescent images. For comparison, all images were taken with the shallower grooves in parallel to the x axis. In general, both cell shape and nucleus morphology can be taken as the assessment criteria for cell alignment analysis. In our work, as the NIH 3T3 cells would have two or more extending regions with different direction angles, it is hard to define the cell alignment via the cell shape, and the nucleus morphology was used for image analyses representing the alignment of cells, as the nucleus is mechanically integrated with the physical entity of the cell via intermediate filaments.[15] Since the measured angles between 90 and 180° describe the same cell alignment direction as those between 0 and 90°, the measured angles (0−180°) were converted into a range between 0 and 90°, and then the average angles were obtained to represent the cell alignment degree.

NIH 3T3 cells were observed to respond to the multidirectional patterns in a highly sensitive manner. As expected, the morphology of cells was altered depending on spacing and depth of the groove. In general, the protrusions of cells are along the grooves 20 h after seeding, while they randomly spread on a flat surface.

Figure 4 shows SEM of regular two-level patterns and corresponding fluorescence images of cells as well as angle distribution of the major axis of NIH 3T3 cells. Here, the spacing of the shallow grooves was fixed (8 μm) whereas that of

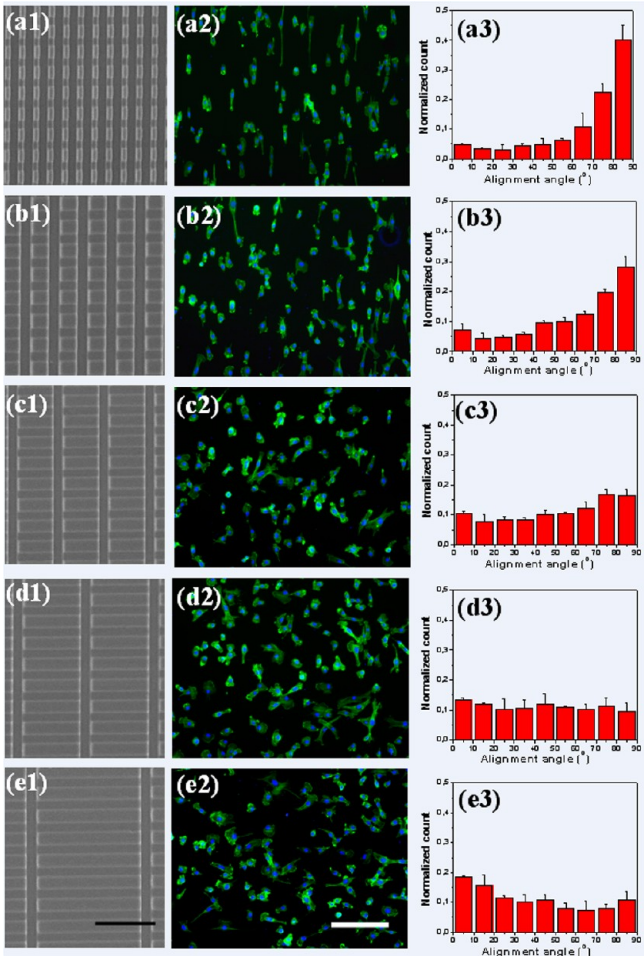

Figure 4. Contact guidance of NIH 3T3 cells on two-level crossing grooves with the same pitch size in one direction (8 μm, top level) but different pitch sizes in another direction (4 to 52 μm, bottom level) . (a1−e1) SEM images of the fabricated patterns. (a2−e2) Fluorescence microscope images of cultured NIH 3T3 cells 20 h after seeding; higher magnification images can be seen in Supporting Information Figure S1. (a3−e3) The distributions of cell alignment angles of NIH 3T3 cells, showing a strong pattern size and type dependence. Scale bar: (a1−e1) 30 μm, (a2−e2) 100 μm.

the deeper grooves varies in the range between 4 and 48 μm. Cells were considered aligned along the deep grooves (bottom level) if the angle between the cell major axis and the deep groove was less than 10°. Clearly, the pitch size of the deeper grooves has more important effects on cell alignment. When the pitch size of the deeper grooves was small (4 μm, Figure 4a1−a3), around 40% of the cells was oriented along the direction of deeper grooves. When the pitch size of the deeper grooves was the same as that of the shallower ones, cells were still likely to orient along the direction of deeper grooves (Figure 4b1−b3). When the pitch size of the deeper grooves was much larger than that of cells, however, cells were elongated along the shallower grooves (Figure 4e1−e3). In other cases, the effects of cell elongation and alignment were determined by the competition between deeper (with larger pitch size) and shallower (with smaller pitch size) ones (Figure 4c1−c3,d1−d3). The measured average angles (θ) between the cell major axis and the direction of the x axis (shallow grooves) also changed regularly with the change of the groove depth and pitch size (see the Supporting Information Table S1). These results strongly suggested that the influences of the groove depth and pitch size are closely correlated.

Patterns down to submicrometer and nanometer scales have also a strong effect on cell alignment.[25,26] However, when they were superimposed on microgrooves and surface coated with adhesion molecules (FN at concentration of 25 μg/mL), the effect on cell alignment could be reduced. It seems that such a decrease was more significant ($p < 0.05$) with superimposed submicrometer pits compared to other types of patterns in submicrometer scale (pillars, gratings parallel or perpendicular to the grooves, the data are provided in Supporting Information Table S2). The measured average angles (θ) between the cell major axis and the direction of the grooves were 24.4 ± 2.83 (22.19 ± 0.77), 31.61 ± 0.64 (30.15 ± 0.72), 35.26 ± 3.33 (31.3 ± 1.9), and 44.2 ± 1.39 (39.18 ± 0.88), respectively, for the grooves of pitch size of 4, 8, 16, and 32 μm with (without) submicrometer pits on the groove ridges. It can therefore be suggested that the pits in submicrometer scale on the groove ridges have the effect to decrease the contact guidance of microgrooves. However, this effect becomes less important with the increase of the groove depth.

In summary, we have developed a novel and simple fabrication technique of two-level topographic patterns, which allows for the fabrication of dual-level patterns with different depths and imposed submicrometer features on microsized patterns in various combinations, for observation of competitive guidance of cell alignment. Although further studies such as the identification of the nucleus or cell morphology on deep and shallow grooves, as well as on groove ridges, need to be addressed to elucidate the mechanism of this competitive guidance, both the fabrication technique and the findings in this work will enable us to enhance our knowledge in describing substrate mediated cellular regulation and cultivation of cell sheets for the regenerative medicine, benefiting not only the fundamental biology but also the field of tissue engineering.

CONCLUSIONS

A simple but yet robust method has been developed for manufacturing two-level topographical cues for cell alignment studies. The crossing microgrooves with different depths and spacing, as well as superimposed nanostructures on the top of groove ridges, were produced, showing competitive effects of contact guidance for cells at different length scales. This study demonstrated that multilevel topographic cues can be exploited to control cell culture behaviors. This technique could be translated directly to other types of adhesive cells and/or more sophisticated patterns, thereby providing a way to optimize the culture substrates for in vitro cell biology studies.

ASSOCIATED CONTENT

Supporting Information

Fluorescence microscope images and tables showing average alignment angles. This material is available free of charge via the Internet at http://pubs.acs.org.

AUTHOR INFORMATION

Corresponding Author

*Tel.: +33 1 44322421. Fax: +33 1 44322402. E-mail: yong.chen@ens.fr (Y.C.), jianshi@ens.fr (J.S.).

Notes

The authors declare no competing financial interest.

■ ACKNOWLEDGMENTS

This work was supported by European Commission through project contract IRSES-GA-2009-247641 (Microcare) and Japan Society for Promotion of Science through project contract JSPS, Nos. 22350104 and 22710116. The content of this work is the sole responsibility of the authors.

■ REFERENCES

(1) Hahn, M. S.; Miller, J. S.; West, J. L. *Adv. Mater.* **2006**, *18*, 2679−2684.
(2) Ingber, D. E.; Mow, V. C.; Butler, D.; Niklason, L.; Huard, J.; Mao, J.; Yannas, I.; Kaplan, D.; Vunjak-Novakovic, G. *Tissue Eng.* **2006**, *12*, 3265−3283.
(3) Flemming, R. G.; Murphy, C. J.; Abrams, G. A.; Goodman, S. L.; Nealey, P. F. *Biomaterials* **1999**, *20*, 573−588.
(4) Cai, N.; Wong, C. C.; Gong, Y. X.; Tan, S. C. W.; Chan, V.; Liao, K. *ACS Appl. Mater. Interfaces* **2010**, *2*, 1038−1047.
(5) Lutolf, M. P.; Hubbell, J. A. *Nat. Biotechnol.* **2005**, *23*, 47−55.
(6) Moroni, L.; Schotel, R.; Hamann, D.; de Wijn, J. R.; van Blitterswijk, C. A. *Adv. Funct. Mater.* **2008**, *18*, 53−60.
(7) Gadegaard, N.; Dalby, M. J.; Riehle, M. O.; Curtis, A. S. G.; Affrossman, S. *Adv. Mater.* **2004**, *16*, 1857−1860.
(8) Shi, J.; Wang, L.; Zhang, F.; Li, H.; Lei, L.; Liu, L.; Chen, Y. *ACS Appl. Mater. Interfaces* **2010**, *4*, 1025−1030.
(9) Walboomers, X. F.; Croes, H. J. E.; Ginsel, L. A.; Jansen, J. A. *Biomaterials* **1998**, *19*, 1861−1868.
(10) Uttayarat, P.; Toworfe, G. K.; Dietrich, F.; Lelkes, P. I.; Composto, R. J. *J. Biomed. Mater. Res. A* **2005**, *75A*, 668−680.
(11) Lim, J. Y. *Tissue Eng. Regener. Med.* **2009**, *6*, 365−370.
(12) Bettinger, C. J.; Langer, R.; Borenstein, J. T. *Angew. Chem., Int. Ed.* **2009**, *48*, 5406−5415.
(13) Théry, M.; Racine, V.; Pépin, A.; Piel, M.; Chen, Y.; Sibarita, J. B.; Bornens, M. *Nat. Cell Biol.* **2005**, *10*, 947−953.
(14) Yim, E. K. F.; Reano, R. M.; Pang, S. W.; Yee, A. F.; Chen, C. S.; Leong, K. W. *Biomaterials* **2005**, *26*, 5405−5413.
(15) Sniadecki, N. J.; Desai, R. A.; Ruiz, S. A.; Chen, C. S. *Ann. Biomed. Eng.* **2006**, *34*, 59−74.
(16) Geiger, B.; Bershadsky, A.; Pankov, R.; Yamada, K. M. *Nat. Cell Biol.* **2001**, *2*, 793−805.
(17) Mai, J.; Sun, C.; Li, S.; Zhang, X. *Biomed. Microdevices* **2007**, *9*, 523−531.
(18) Jeon, H.; Hidai, H.; Hwang, D. J.; Healy, K. E.; Grigoropoulos, C. P. *Biomaterials* **2010**, *31*, 4286−4295.
(19) Kim, D. H.; Seo, C. H.; Han, K.; Kwon, K. W.; Levchenko, A.; Suh, K. Y. *Adv. Funct. Mater.* **2009**, *19*, 1579−1586.
(20) Nikkhah, M.; Edalat, F; Manoucheri, S.; Khademhosseini, A. *Biomaterials* **2012**, *33*, 5230−5246.
(21) Michel, R.; Reviakine, I.; Sutherland, D.; Fokas, C.; Csucs, G.; Danuser, G.; Spencer, N.; Textor, M. *Langmuir* **2002**, *18*, 8580−8586.
(22) Klein, F.; Striebel, T.; Fischer, J.; Jiang, Z.; Franz, C. M.; von Freymann, G.; Wegener, M.; Bastmeyer, M. *Adv. Mater.* **2010**, *22*, 868−871.
(23) Sun, M. H.; Luo, C. X.; Xu, L. P.; Ji, H.; Ouyang, Q.; Yu, D. P.; Chen, Y. *Langmuir* **2005**, *21*, 8978−8981.
(24) Zhou, X. T.; Zhang, F.; Hu, J.; Li, X.; Ma, X. M.; Chen, Y. *Microelectron. Eng.* **2010**, *87*, 1439−1443.
(25) Hu, J.; Shi, J.; Zhang, F.; Lei, L.; Li, X.; Wang, L.; Liu, L.; Chen, Y. *Microelectron. Eng.* **2010**, *8*, 726−729.
(26) Kim, D. H.; Lipke, E. A.; Kim, P.; Cheong, R.; Thompson, S.; Delannoy, M.; Suh, K. Y.; Tung, L. M.; Levchenko, A. *Proc. Natl. Acad. Sci. U.S.A.* **2010**, *107*, 565−570.